Journal Pre-proof

Determination of mercury at picogram level in natural waters with inductively coupled plasma mass spectrometry by using 3D printed metal scavengers

Suvi Kulomäki, Elmeri Lahtinen, Siiri Perämäki, Ari Väisänen

PII: S0003-2670(19)31176-6

DOI: https://doi.org/10.1016/j.aca.2019.09.075

Reference: ACA 237128

To appear in: *Analytica Chimica Acta*

Received Date: 13 June 2019

Revised Date: 20 September 2019

Accepted Date: 26 September 2019

Please cite this article as: S. Kulomäki, E. Lahtinen, S. Perämäki, A. Väisänen, Determination of mercury at picogram level in natural waters with inductively coupled plasma mass spectrometry by using 3D printed metal scavengers, *Analytica Chimica Acta*, https://doi.org/10.1016/j.aca.2019.09.075.

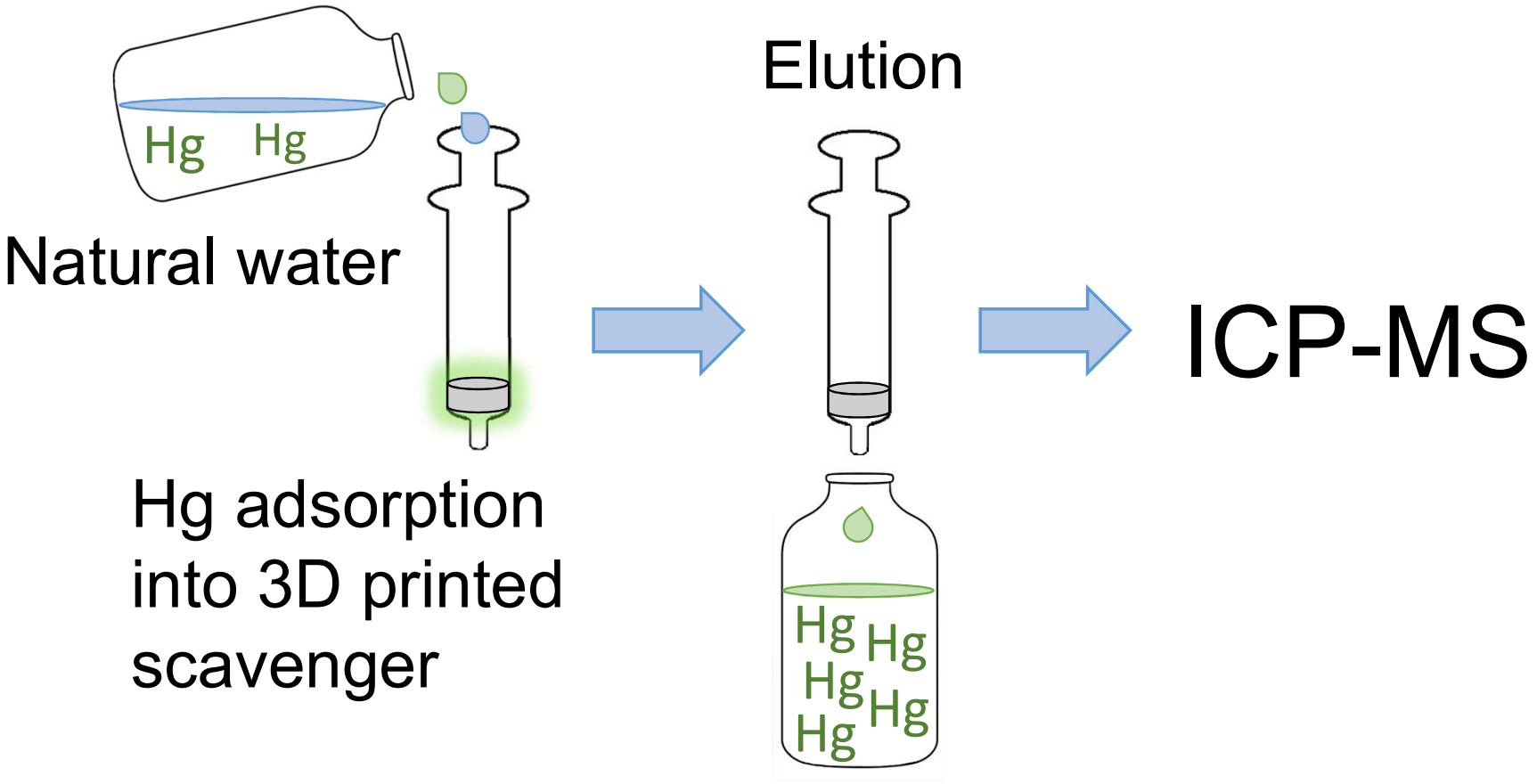
Hg Hg
Natural water
Hg adsorption into 3D printed scavenger
Elution
Hg Hg Hg Hg Hg
ICP-MS

Determination of mercury at picogram level in natural waters with inductively coupled plasma mass spectrometry by using 3D printed metal scavengers

Suvi Kulomäki*, Elmeri Lahtinen, Siiri Perämäki, Ari Väisänen

Department of Chemistry, Renewable Natural Resources and Chemistry of Living Environment, University of Jyväskylä, P.O. Box 35, FI-40014 Jyväskylä, Finland

Abstract

The determination of ultra-trace concentrations of Hg in natural water samples via preconcentration using 3D printed metal scavenger technique followed by inductively coupled plasma mass spectrometry (ICP-MS) was developed. The determination of Hg in certified reference material ERM-CA615 (groundwater) was performed with high accuracy and precision resulting in recovery of 100 ± 3% and RSD <2.5%, respectively. Selective laser sintering (SLS) 3D printing was used to fabricate the scavengers using a mixture of polyamide-12 powder with thiol-functionalized silica. The preconcentration procedure is based on the adsorption of the Hg on the scavenger and followed by elution of the preconcentrated Hg from the filter with 0.3% thiourea in 8% HCl prior to its determination by ICP-MS. A preconcentration factor of 92.8 can be achieved by filtering 495 mL of water followed with the elution step. Very low instrumental detection limit and method detection limits were obtained resulting in 0.013 and 0.037 ng L^{-1}, respectively. The method was applied successfully for the determination of Hg in different lake and river water samples. The developed method is the first preconcentration method enabling simple and accurate determination of Hg in pg L^{-1} concentrations in natural waters with ICP-MS.

Keywords: Mercury; Inductively coupled plasma mass spectrometry; Ultra-trace concentration; Preconcentration; 3D printing; Natural water.

*Corresponding Author. E-mail address: suvi.t.kulomaki@jyu.fi (S. Kulomäki)

1. Introduction

Mercury is one of the most toxic elements due to its accumulative and persistent nature in the environment and living organisms. It occurs naturally in the environment in a variety of chemical and physical forms at very low concentrations [1]. In pristine natural waters, Hg concentrations are typically between pg and ng L^{-1} range. Recent reports estimate a total mercury concentration in natural waters ranging from 0.03 to 90 ng L^{-1}, while contaminated waters may contain up to several µg L^{-1} of Hg [1,2]. Although mercury is not an abundant element in nature, its presence in polluted waters and the uptake of Hg by aquatic media has become an area of great environmental concern and a potential risk to human health [3]. All forms of mercury are poisonous and its toxicity is generally increased by transformation into organic forms via biomethylation [1]. Monitoring of mercury traces in the hydrosphere has been regulated in many countries, e.g., in Europe by the European Water Framework Directive [2,4]. Hg is included in Annex I of the Directive 2013/39/EU as priority hazardous substance and a maximum allowable concentration of Hg and its compounds of 0.07 µg L^{-1} in inland and other surface waters has been established [5,6]. In Finland, heavy metal concentrations in natural waters are usually at a very low level. For this reason, the method detection limits for Ni, Cd, Pb, and Hg are stricter than those presented in the Water Framework Directive. For Hg, the recommendation for method detection limit is 5 ng L^{-1} [7].

Accurate quantification of Hg traces in natural waters is challenging due to very low Hg concentrations. Highly sensitive detection techniques are available for mercury e.g. cold vapor atomic fluorescence spectrometry (CV-AFS) and inductively coupled plasma mass spectrometry (ICP-MS) but most modern analytical techniques do not succeed in direct determination of low Hg concentrations [1,2,8]. Thus, a preconcentration step is needed to reach the detection limits required for the environmental monitoring of Hg [9]. The analytical performance of non-chromatographic methods using different types of preconcentration

methods has been reviewed previously [1,10,11]. Most of these methods are using a tedious cold vapor generation coupled to atomic spectroscopic techniques with detection limits between 0.05 and 500 ng L^{-1} for Hg^{2+}. Still, many of these approaches have inadequate detection limit for ultra-trace Hg analysis in environmental samples and the development of simple and sensitive methods are highly desirable.

During the preconcentration step, the analyte is usually also separated from most of the matrix elements, in order to eliminate possible interferences and lowering the detection limit [12]. Various approaches have been applied for separation and preconcentration of Hg based mainly on liquid-liquid extraction [13–15], co-precipitation [16,17] and solid-phase extraction (SPE) [3,6,18–20]. SPE is the most commonly used preconcentration method for trace metals due to its simplicity, flexibility, and ability to achieve high enrichment factors. Extraction efficiency and selectivity are greatly dependent on the sorbent material used and therefore the choice of the appropriate adsorbent with high affinity and selectivity for Hg is the most critical step in SPE method development [12]. Numerous materials, such as chelating resins [21], ion exchangers [22–24], modified carbon nanotubes [25,26] and nanoparticles [2,3], modified silica gel [27] and polyurethane foam [28,29] have been suggested as SPE sorbents. There are also some commercially available metal scavengers for Hg but their disadvantage is that they are usually sold as powdery materials and hence centrifugation or filtration is needed to recover the used adsorbent or to purify the sample solutions from remaining particles. These difficulties make the use of the adsorbent laborious and challenging. Moreover, the use of solid samplers instead of small particle material would enable in situ sampling which would be almost impossible with a material consisting of small particles. These challenges can be avoided by anchoring the chemically active component to a sorbent matrix by using 3D printing.

Over the past few years, 3D printing has received increasing attention as a way to fabricate macroscopic objects with actual functionality instead of just mechanical or aesthetical properties [30–35]. 3D printing has found many potential applications in the fields of separation sciences [36] and analytical chemistry [37]. However, many of these reports have been focusing on either extrusion-based methods or stereolithography whereas methods such as Selective Laser Sintering (SLS) have received less attention. This is even though the SLS 3D printing possesses some obvious advantages if targeting, for example, any kind of flow-related processes. The challenge with the aforementioned extrusion-based and stereolithography methods is that they produce objects, where the surfaces of the printed objects are completely solid and the reactive surface area inside the object is not accessible.

The SLS 3D printing doesn't suffer from similar challenges as it uses a laser to partially sinter small polymer beads together, leaving accessible voids between the polymer particles. These voids are crucial for analytical chemistry purposes, as they allow the fluid to flow through the pores of the objects and therefore allow for controlled chemical interaction between the fluid and the object. This level of sintering, and therefore the porosity, can be controlled by adjusting the printing parameters such as laser power, laser speed and temperature [38–41]. Even different areas of the same object can be made to possess different porosities. For example, the outer walls of the object can be made impermeable for fluids while leaving the inside of the object highly macroporous [42]. The chemical functionality can be embedded into the printed objects either by simply mixing the additive into the starting material or by post-processing the printed objects. Almost anything can be used as the additive since as long as the additive can withstand the temperature of the printing process, it can be printed to form chemically functionalized macroscopic objects without losing the activity of the additive during the process [42,43]. Turning powdery materials into

easily handleable objects with customizable shape, size and porosity often make their use in actual applications much more feasible if compared to using them in their powdery form.

This paper presents a 3D printed Hg scavenger (3D-Thiol) method for the preconcentration and determination of ultra-trace mercury concentrations in natural waters. A series of sorption experiments were conducted using flow-through procedures to study the effect of sorption, elution, and selectivity for mercury and some other metals. In addition, adsorption isotherms for thiol functionalized silica (Thiol) and 3D-Thiol were determined. Finally, an analytical method for Hg determination in ultra-trace concentrations was developed, based on sorption of Hg on 3D-Thiol and elution using HCl and thiourea solution followed by ICP-MS detection. To our knowledge, this is the very first study enabling Hg detection with ICP-MS for pg L^{-1} concentrations without the utilization of cold vapor technique. In addition, this is the first instance where thiol functionalized material, use-case and functionality have been combined with SLS 3D printing.

2. Experimental Section

2.1. Reagents

All reagents were of analytical grade and all aqueous solutions were prepared in high purity water (18.2 MΩ cm) produced by Elga Purelab Ultra water purification system (Buckinghamshire, U.K.). Single-element standard of Hg as Hg^{2+} (10 mg L^{-1}, PurePlus), Cd, Co, Cr, Fe, Ir, K, Mg, Mn, Na, Ni, and Pb (1000 mg L^{-1}, Pure) were supplied by PerkinElmer. 1000 mg L^{-1} stock solution of Ca was prepared from $CaCO_3$ (Merck, ≥99.0%). The ICP-MS performance was checked daily with a NexION Setup Solution (1 μg L^{-1} Be, Ce, Fe, In, Li, Mg, Pb, and U in 1% HNO_3, PerkinElmer). Thiourea (99.8%) was obtained from VWR Chemicals and SiliaMetS Thiol was purchased from SiliCycle (Quebec City, Canada). Polyamide-12 (PA12), thermoplastic polyurethane and polypropylene printing powders were

purchased from BASF (Ludwigshafen am Rhein, Germany). Certified reference material (ERM-CA615, groundwater) was produced and certified by the Joint Research Centre, Institute for Reference Materials and Measurements (JRC-IRMM). Ultra-pure hydrochloric acid (34–37%) was purchased from ANALYTIKA, spol. s r.o. (Prague, Czech Republic). Puriss. p.a. hydrochloric acid (≥37%) and nitric acid (≥65%) were purchased from Merck and were used for wash solutions with ESI prepFAST. All glass containers that could come into contact with samples and standards were filled with 10% (v/v) hydrochloric acid (≥37%) for at least 24 h and tested for Hg followed by ICP-MS analysis. Sample bottles were first rinsed thoroughly with ultrapure water and then completely filled with it. A blank sample was prepared by using this water and was then analyzed with ICP-MS. Sample bottles were used if the measured Hg concentration was below the instrument detection limit (IDL). After testing, glass containers were filled with dilute HCl (~0.5%) and were thoroughly rinsed with high purity water before usage. Calibration standards and smaller volume samples were prepared into 50 mL polypropylene centrifuge tubes (VWR International).

2.2. Sampling and sample pretreatment

A total of seven different water samples were collected in 2L glass bottles from central Finland. Tap water was collected from the research laboratory of the Department of Chemistry (Jyväskylä), groundwater from Heinäahonlähde (Laukaa), Lake water 1 from lake Päijänne (Korpilahti), Lake water 2 from lake Jyväsjärvi (Jyväskylä), River water from river Tourujoki (Jyväskylä), Pond water 1 from Myllylampi (Tikkakoski) and pond water 2 from Mustalampi (Jyväskylä). Samples were filtered (Whatman No. 41) only if they contained solid material. Then they were acidified with ultra-pure HCl to obtain 3% (v/v) acid concentration and stored at 4 °C in a refrigerator overnight if not analyzed immediately after the sample collection.

2.3. Instrumentation

All mercury analyses were performed on a PerkinElmer (Massachusetts, U.S.A.) NexION 350D inductively coupled plasma mass spectrometer (ICP-MS) in standard mode. The ICP-MS was interfaced with an Elemental Scientific (Nebraska, U.S.A.) prepFAST 4DX sample/standard autodilution system. A NexION Setup Solution was used for the daily optimization procedures for the ICP-MS according to manufacturer's instructions. Data were acquired in counts per second (cps) for Hg (the sum of the counts at *m/z* 200, 201 and 202), and Ir (*m/z* 193) was used as the internal standard. The most abundant W isotope ^{184}W was monitored during all measurements, and it was concluded that WO did not interfere with Hg in the studied water samples when the 3D-Thiol method was used. Calibration standards were prepared in the range of 0–500 ng L^{-1} (blank, 50, 250 and 500 ng L^{-1}) Hg and the standards and samples were adjusted to contain 3% (v/v) HCl. For analysis of elution solutions containing thiourea and HCl, the standards were matrix-matched with 0.1125% (m/v) thiourea and 3% (v/v) HCl. The system was first rinsed with a mixture of 0.75% (v/v) HNO_3 and 2.25% (v/v) HCl and then with 3% (v/v) hydrochloric acid between samples. The optimum operating conditions and measurement parameters for ICP-MS are listed in Table 1.

Elements present in the selectivity study were analyzed on Avio 500 ICP-OES (PerkinElmer, Massachusetts, U.S.A.) or with ICP-MS. More detailed information about the analytical procedure is presented in Tables S1 and S2. Black/white 3.18 mm i.d. PVC peristaltic pump tubing (PerkinElmer, Massachusetts, U.S.A.) was used for the preconcentration process and the flow rate of the samples was adjusted using an ISCO (Nebraska, U.S.A.) WIZ peristaltic pump. Helium imaging was performed with Carl Zeiss (Oberkochen, Germany) ORION NanoFab helium ion microscope (HIM). The beam energy was set to around 30 kV while the beam current varied between 0.211 and 0.234 pA. Scan dwell time of 0.2 µs with a viewing distance of 5.101 to 7.833 millimeters was utilized for the imaging. Flood gun was used

throughout the imaging to counteract the charging event present. Samples did not receive any additional pretreatment before the imaging process.

2.4. Designing and preparation of the 3D printed scavengers

The objects were designed using FreeCad v. 0.16 and then sliced with Slic3r v. 1.2.9 into 100 µm layers to obtain filters with desired shape and size (5 mm tall disc with 16.5 mm diameter). The starting material for the SLS 3D printing was made by mixing polyamide-12 powder (~50 µm diameter) with either 5 or 10 wt% of thiol-functionalized silica (40–63 µm). The material was then mechanically mixed and placed into the 3D printer. The actual printing process was done using Sharebot SnowWhite SLS 3D printer with a laser power of 30–40% (of a maximum of 14 W), a laser speed of 1800–2400 mm s^{-1} and printing temperature of 170 °C. No post-processing, aside for cleaning the objects of any unsintered powder, was done for the 3D printed objects.

2.5. Adsorption Experiments

The developed 3D-Thiol method was tested with model solutions prior to the separation and preconcentration of Hg from real samples. For this purpose, 3D printed filters were placed into a 10 mL syringe (Fig. 1) and washed from any unsintered powder with ultrapure water. Extraction of Hg from aqueous solutions was investigated in a flow-through process. The sorption was performed in centrifuge tubes containing 100 ng L^{-1} of Hg in 40 mL of 3% (v/v) HCl. Initial tests were carried out using a peristaltic pump with a maximum flow rate (~8.3 mL min^{-1}). The adsorbed concentration of Hg was determined using ICP-MS. Adsorption percentage was calculated using the following equation:

$$\text{Adsorption\%} = \frac{C_{A-}\, C_B}{C_A} \cdot 100\% \qquad (1)$$

where C_A and C_B are initial and final concentration (ng L^{-1}) in the solution, respectively [44]. In the elution step, 2–10 mL of 0.3–2% (w/v) thiourea and 8–40% (v/v) hydrochloric acid solution was passed through 3D-Thiol at a flow rate of ~1–8.3 mL min^{-1}.

2.6. Determination of adsorption capacity

Equilibrium isotherm studies were carried out with different initial concentrations of Hg in flow-through experiments. The adsorption capacity was determined for both Thiol and 3D-Thiol. The adsorption efficiency of Thiol was performed by adding 10 mg of beads into 40 mL of different solutions containing different concentrations of Hg (1, 25, 50, 75 and 100 mg L^{-1}) in 3% (v/v) HCl. The tube was sealed and then agitated using Stuart SF1 at 500 osc min^{-1} for 2 h at room temperature. The thiol-functionalized silica was removed from the Hg solution by filtration (Whatman No. 42) and samples were analyzed by using ICP-MS after appropriate dilution.

The adsorption capacity for 3D-Thiol was performed with the same sample volume and Hg concentrations as above. To obtain approximately 10 mg of Thiol in the printed scavenger, the weight fraction of the additive was dropped to 5 wt% in the printed scavenger and 3D-Thiol filters were placed into a 5 mL syringe. 40 mL solutions were passed through one filter five times with a peristaltic pump at a maximum flow rate (~8.3 mL min^{-1}). After adsorption, the residual concentration of Hg was analyzed by ICP-MS after appropriate dilution. The concentration of Hg adsorbed per unit mass of the adsorbents was calculated from the following equation:

$$q_e = \frac{(C_0 - C_e)V}{m} \qquad (2)$$

where q_e is the adsorption capacity (mg g^{-1}) of the adsorbent at equilibrium; C_0 and C_e are the initial and final concentration of Hg (mg L^{-1}), respectively; V is the volume of the solution (L) and m is the mass of the adsorbent (g).

2.7. Selectivity experiments

A variety of 40 mL samples containing spiked lake water or synthetic sample were passed through a 10 ml syringe containing one 3D-Thiol filter with a ~8.3 mL min^{-1} flow rate. Spiking levels were 5 ng L^{-1} of Hg, 10 mg L^{-1} of Ca, 6 mg L^{-1} of Na, 2 mg L^{-1} of Mg, 1 mg L^{-1} of K, 1 mg L^{-1} of Fe and 50 µg L^{-1} of Cd, Co, Cr, Mn, Ni, and Pb. Ca, Na, Mg, K, Fe, Cr, and Mn were measured with ICP-OES and Co, Ni, Cd, Pb, and Hg were analyzed with ICP-MS. More detailed information about the analytical procedure is presented in Table S3.

2.8. Spiking studies and the treatment of the real sample

Samples were spiked with 20 ng L^{-1} of Hg and prepared in 45 mL volume of which 5 ml was set aside for direct ICP-MS analysis. The real samples were prepared into 500 mL volume and 5 mL of the sample was saved for direct measurement with ICP-MS. The sample solution was pushed through the 3D-Thiol with ~5 mL min^{-1} flow rate using a peristaltic pump resulting in the time needed for preconcentration to be about 1 h 40 min. The elution step was done without a peristaltic pump in backflush mode. The retained Hg was eluted with 2 mL of 0.3% (w/v) thiourea in 8% (v/v) HCl solution. The syringe plunger was used to gently push the first drop of the eluent through 3D-Thiol. Then the rest of the eluent was allowed to drain through the filter. Finally, the 3D-Thiol was washed with 3.335 mL of ultrapure water to obtain 3% (v/v) HCl concentration in the final solution, which was analyzed by ICP-MS. The elution and washing take approximately 5 minutes.

3. Results and discussion

3.1. Analytical performance of ICP-MS analysis

The method showed good linearity over the calibration range of 0–500 ng L^{-1} (Fig. S1) and the correlation coefficient of linear regression (r^2) was higher than 0.9999. IDL achieved for Hg determination was 1.2 ng L^{-1} (calculated as three times the standard deviation of a series of 10 replicate measurement of the calibration blank). The method detection limit (MDL) was determined according to U.S Environmental Protection Agency method detection limit procedure [45] and it was calculated to be 3.5 ng L^{-1}. The short and long term precision were estimated by measuring a quality control sample containing 20 ng L^{-1} of Hg, 20 mg L^{-1} of C, 5 mg L^{-1} of Ca, 1 mg L^{-1} of Fe, 2 mg L^{-1} of K, 2 mg L^{-1} of Mg and 5 mg L^{-1} of Na and 2 mg L^{-1} of S. The precision (relative standard deviation, RSD) within one day was 2.9% (n=7) and during four weeks 4.0% (n=23). In addition, the precision and accuracy of the ICP-MS method were estimated using a certified groundwater reference material (ERM-CA615, certified value 37 ± 4 ng L^{-1}; expanded uncertainty at 95% confidence level). Replicate analyses on two different days gave a mean value of 37.0 ng L^{-1} (n = 5) with a precision of 2.5%.

3.2. Selection of the chemically active component and supporting matrix

Several commercially available metal scavengers and ion exchange materials were examined for the preconcentration of Hg. Thiol-functionalized silica proved to be the most suitable scavenger for Hg so it was chosen for a chemically active component for 3D printed scavenger. Resins containing the thiol functional groups have been found to be able to adsorb Hg [46,47]. Unfortunately, many of these are no longer commercially available (Spheron-Thiol, Duolite GT73, Ambersep GT74). Polyamide-12, thermoplastic polyurethane, and polypropylene printing powders were tested for 3D printing supporting matrix. PA12 proved

to be a suitable material since it is a readily available, durable and easily printable polymer. In addition, Hg was not retained by the PA12 after elution with acidic thiourea solution.

3.3. Macroscopic structure of the 3D printed filter

The HIM imaging was used to get information about the macroscopic structure of the printed object as well as the distribution and the attachment of the additive. HIM imaging, instead of the more traditional SEM imaging, was conducted for the printed filters to combat the charging effect often when imaging nonconductive samples [48]. It is also evident, that the silica particles have not been capsulated by the polymer and therefore they remain accessible for chemical reactions (Fig. 2 left). The overall structure of the printed filter can be seen to be highly macroporous, consisting of polymeric beads that have been partially sintered together by the laser during the printing process. Additionally, the distribution of the silica particles throughout the printed object seems to be rather even (Fig. 2 right). However, this was expected as the distribution and the attachment for a similar system has been previously reported [42,43] and thus was not studied more in depth here.

3.4. Adsorption and adsorption isotherm studies

Initial adsorption experiments were conducted using a peristaltic pump. During the experiment, up to 97% of the Hg was adsorbed, which shows the rather satisfactory retention kinetics. Complete adsorption could be achieved with a more moderate flow rate (~5 mL min^{-1}). In this case, the Hg concentration in the remaining solution is very close or below the instrument detection limit (1.2 ng L^{-1}) which indicates complete adsorption. Since the Hg concentration in pristine natural waters can be only a few ng L^{-1}, a high preconcentration factor is desired. The preconcentration factor can be maximized by increasing the sample volume and decreasing the eluent volume. However, due to practical reasons such as ease of sampling and duration of pretreatment, the volume of real natural water sample should be

kept reasonable. Taking these considerations into account, a sample volume of 500 mL was chosen, of which 5 mL was set aside for direct ICP-MS analysis.

The equilibrium conditions of the sorption process can be described using sorption isotherms. The most frequently used adsorption isotherm equations [23,49,50] of the Langmuir (3) and Freundlich (4) isotherms were applied to utilize the linearized equations indicated below:

$$\frac{C_e}{q_e} = \frac{1}{K_L \cdot q_{max}} + \frac{C_e}{q_{max}} \qquad (3)$$

$$\ln q_e = \ln K_F + \frac{1}{n} \ln C_e \qquad (4)$$

where q_e (mg g^{-1}) is the equilibrium adsorption capacity, C_e (mg L^{-1}) is the Hg concentration at equilibrium, q_{max} (mg g^{-1}) is the monolayer maximum adsorption capacity, K_L (L mg^{-1}) is Langmuir equilibrium constant, K_F (L g^{-1}) is a coefficient related to the amount of adsorbed metal ions and n is Freundlich adsorption constant related to surface heterogeneity. The Langmuir equation assumes the same energy for all adsorption sites and that monolayer is formed when the solid surface reaches saturation [51]. The plot of C_e/q_e against C_e gives a straight line and the values of q_{max} and K_L are obtained from the slope and intercept of the plot [23]. The Freundlich isotherm, in turn, is an empirical equation and assumes that adsorption is multilayer and is based on heterogeneous surface adsorption suggesting that binding sites are not equivalent [23,51].

Linear plots of $\ln q_e$ versus $\ln C_e$ revealed that the adsorption obeys well Freundlich isotherm (Fig. S2). The results showed that the Hg adsorption onto Thiol can be considered to be a multilayer adsorption system (Table 2). The loading capacity for Thiol is 264.8 mg g^{-1} according to the manufacturer. The experimental value obtained from the Langmuir isotherm model for Thiol was 253.5 mg g^{-1} and for 3D-Thiol 222.4 mg g^{-1}. These results indicate that 3D printing decreases the maximum capacity of the resin only slightly. Hg concentrations in

natural waters are so low that the maximum loading capacity is not easily reached. For example, Hg concentration of 46 mg L^{-1} with a sample volume of 500 mL is required to saturate all absorption sites of 3D-Thiol.

3.5. Selectivity

In order to study the selectivity of 3D-Thiol towards Hg, competitive adsorption of Ca, Cd, Co, Cr, Fe, K, Mg, Mn, Na, Ni, and Pb from spiked lake water and synthetic sample were investigated. In spite of the high concentrations of other metal ions (0.05–10 mg L^{-1}), Hg was retained to 3D-Thiol completely as the Hg concentration of the sample that passed through the filter was below the limit of detection. Moreover, Ca, Na, Mg, K, Cr, and Mn were not retained at all, Fe, Co, Ni, Cd, and Pb showed very low percentage retention values to be ≤ 1.0% (Table S4). 3D-Thiol proved to be extremely selective for Hg in 3% (v/v) HCl. These results provide further evidence of the great selectivity of 3D-Thiol for Hg.

3.6. The effect of eluent composition and its volume

According to initial testing with different eluents and literature review [1,52,53], thiourea in hydrochloric acid solution was found to be the most promising eluent. HCl has also been reported [54] to have an enhanced performance due to its complexing abilities with mercury and therefore it was of interest to investigate the influence of thiourea and HCl concentration on the elution efficiency for 3D-Thiol. Thiourea was found to affect the intensity level of the internal standard in ICP-MS analysis, hence, the samples with different eluent compositions were analyzed without internal standard correction (Table 3). To enable the use of internal standard, matrix matching was employed in subsequent analysis.

Effect of thiourea and HCl concentration on elution efficiency was studied in duplicates with 10 mL eluent volumes and ~8.3 mL min^{-1} flow rate without internal standard correction (Table 3). Higher thiourea and acid concentration results in complete elution of Hg from the

3D-Thiol, however, it is desirable to keep the acid concentration and total dissolved solids below 4% and 0.2%, respectively for ICP-MS [55]. Samples have to be diluted before measurement if the acid concentration is above the tolerable limits and hence the higher preconcentration factor would be lost. In addition, at least 4 mL sample volume is needed for measurement. Because of these reasons, 0.3% thiourea in 8% HCl was chosen for further studies.

The effect of eluent volume (2, 5 and 10 mL) and eluent flow rate (~1, 3 and 5 mL min^{-1}) were evaluated using a peristaltic pump with the selected eluent. It was observed, that the recovery was satisfactory (98–110%) with all tested eluent volumes and flow rates. However, these small eluent volumes were not completely recovered when using a peristaltic pump. To obtain quantitative recoveries, the elution step was performed manually without a peristaltic pump as described in section 2.8. Considering the sample volume of 495 mL, final elution volume of 2 mL and a dilution factor of 2.67, the preconcentration factor becomes 92.8. The method detection limit for 3D-Thiol method becomes 0.037 ng L^{-1} when the preconcentration factor is taken into account.

3.7. Reusability of the sorbent

The reusability of 3D-Thiol as a sorbent was examined by assessing the change in the recoveries of the analyte through several sorption-elution cycles at a maximum flow rate of the peristaltic pump following the procedure described in section 2.5. The results revealed that one 3D-Thiol filter could be reused up to 10 times without a loss of adsorption efficiency (Fig. S3). The recovery and relative standard deviation throughout the reusability test for adsorption was 95.2% and 0.7%, respectively (n=2). The adsorption was satisfactory even when the highest flow rate was used. As stated previously, the extraction efficiency is easily

increased with a more moderate flow rate. Nonetheless, in order to avoid any contamination, new 3D-Thiol filters were employed throughout the study.

3.8. Spiking tests

A total of five spiked real samples were analyzed with the 3D-Thiol method as well as directly without any preconcentration. The results obtained using 3D-Thiol method were significantly closer to the spiked concentration of 20 ng L^{-1} compared with the direct measurement as can be seen in Table 4. This can be seen more clearly in the case of yellow to brown color waters (Lake water 1, River and Pond water) which contain more humic substances than clearer waters (Tap water and Lake water 1). Some spiking tests were also performed at 10 ng L^{-1} level, for which direct measurement from tap water gave 10.2 ng L^{-1} (RSD 7.2%) and 3D-Thiol method 10.2 ng L^{-1} (RSD 1.7%). It is likely that the challenging matrix of the colored waters suppresses the signal of mercury in direct ICP-MS determination and might result in biased low concentrations (Table 4). With the 3D-Thiol method, Hg can be separated from most of the matrix and interferences are reduced when compared to direct determination. It was observed that RSD values could slightly be improved by using two 3D-filters in the same syringe (Tables 4 and 5). As the amount of the functional group is increased it is more likely that Hg interacts with thiol group and different kind of samples behave in the same manner. Although the RSD values were improved with the use of two 3D-Thiol filters, RSD values were considered to be sufficient even when only one filter was used. Obtained results further confirm the usefulness of the proposed method.

3.9. Analysis of mercury concentration in real samples

The proposed method was applied for the determination of Hg in different water samples. The samples were analyzed both with the direct determination and with the preconcentration method. With direct determination, Hg concentration of the water samples was below the

MDL except for one sample (Table 5). This represents the need for a 3D-Thiol method to enable a reliable analysis of extremely low concentrations of Hg in natural waters. The reproducibility of the method is very good considering the low ng L^{-1} concentrations. In Central Finland, Hg concentrations of natural waters are at a very low level and with the 3D-Thiol method, the recommended 5 ng L^{-1} method detection limit was easily reached.

4. Conclusions

A SLS 3D printed 3D-Thiol scavenger for Hg preconcentration was prepared and applied for the determination of Hg from water samples with ICP-MS. The proposed method offers a simple and highly selective method for the extraction and determination of ultra-trace Hg. 3D-Thiol has an excellent selectivity towards Hg over Ca, Cd, Co, Cr, Fe, K, Mg, Mn, Na, Ni, and Pb. The interfering effects of the matrix are reduced when 3D-Thiol method is applied. In addition, the loading capacity of 222.4 mg g^{-1} for 3D-Thiol is significantly higher than adequate for this application. The captured Hg can be quantitatively eluted from the 3D-Thiol filter with a mixture of 0.3% (w/v) thiourea and 8% (v/v) HCl solution. If desired, the 3D-Thiol scavenger can be reused at least 10 times with no decrease in its extraction efficiency. The results indicate that the new 3D-Thiol is an exceptional candidate for Hg sorption from natural waters. Due to the high preconcentration factor of 92.8 and extremely low detection limit of 0.037 ng L^{-1}, ultra-trace amounts of Hg at pg L^{-1} levels in water samples can be quantified by the method developed.

Acknowledgments

Financially support from the Jenny and Antti Wihuri Foundation is greatly appreciated. The research was also supported by the Department of Chemistry, University of Jyväskylä and by the Technology Industries of Finland Centennial Foundation as a part of The Future Makers program. The authors would like to thank Matti Leppänen and Heidi Ahkola from Finnish

Environment Institute (SYKE) for water samples, Virva Kinnunen, for advice regarding the use of ICP-MS and for water samples and Dr. Kimmo Kinnunen for the HIM imaging.

Appendix A. Supplementary data

Supplementary data to this article can be found online at https://doi.org.

Author Contributions

The manuscript was written through contributions of all authors. All authors have given approval to the final version of the manuscript. S.K. did the Hg adsorption and elution experiments and carried out the ICP-MS and ICP-OES analysis. E.L. prepared the 3D model of the scavenger and performed 3D printing. S.P. assisted in the designing of the experiments and A.V. supervised the project.

References

[1] K. Leopold, M. Foulkes, P. Worsfold, Methods for the determination and speciation of mercury in natural waters—A review, Anal. Chim. Acta. 663 (2010) 127–138. doi:10.1016/j.aca.2010.01.048.

[2] A. Mutschler, V. Stock, L. Ebert, E. Björk, K. Leopold, M. Lindén, Mesoporous Silica-gold Films for Straightforward, Highly Reproducible Monitoring of Mercury Traces in Water, Nanomaterials. 9 (2018) 35. doi:10.3390/nano9010035.

[3] M. Faraji, Y. Yamini, M. Rezaee, Extraction of trace amounts of mercury with sodium dodecyle sulphate-coated magnetite nanoparticles and its determination by flow injection inductively coupled plasma-optical emission spectrometry, Talanta. 81 (2010) 831–836. doi:10.1016/j.talanta.2010.01.023.

[4] European Parliament, Council of the European Union, Directive 2000/60/EC of the European Parliament and of the Council of 23 October 2000 establishing a framework for Community action in the field of water policy, Off. J. Eur. Parliam. L 327 (2000) 1–73.

[5] European Parliament, Council of the European Union, Directive 2013/39/EU of the European Parliament and of the Council of 12 August 2013 amending Directives 2000/60/EC and 2008/105/EC as regards priority substances in the field of water policy, Off. J. Eur. Union. L 226 (2013) 1–17.

[6] M.P. Rodríguez-Reino, R. Rodríguez-Fernández, E. Peña-Vázquez, R. Domínguez-González, P. Bermejo-Barrera, A. Moreda-Piñeiro, Mercury speciation in seawater by liquid chromatography-inductively coupled plasma-mass spectrometry following solid phase extraction pre-concentration by using an ionic imprinted polymer based on methyl-mercury-phenobarbital interaction, J. Chromatogr. A. 1391 (2015) 9–17.

doi:10.1016/j.chroma.2015.02.068.

[7] T. Näykki, T. Väisänen, Laatusuositukset ympäristöhallinnon vedenlaaturekistereihin vietävälle tiedolle. Vesistä tehtävien analyyttien määritysrajat, mittausepävarmuudet sekä säilytysajat ja -tavat. - 2. uudistettu painos, Suom. Ympäristökeskuksen Rap. 22/2016. (2016). http://hdl.handle.net/10138/163532.

[8] A. Zierhut, K. Leopold, L. Harwardt, M. Schuster, Analysis of total dissolved mercury in waters after on-line preconcentration on an active gold column, Talanta. 81 (2010) 1529–1535. doi:10.1016/J.TALANTA.2010.02.064.

[9] K. Leopold, M. Foulkes, P.J. Worsfold, Preconcentration techniques for the determination of mercury species in natural waters, TrAC Trends Anal. Chem. 28 (2009) 426–435. doi:10.1016/j.trac.2009.02.004.

[10] I. Sánchez Trujillo, E. Vereda Alonso, J.M. Cano Pavón, A. García de Torres, Use of a new enrichment nanosorbent for speciation of mercury by FI-CV-ICP-MS, J. Anal. At. Spectrom. 30 (2015) 2429–2440. doi:10.1039/C5JA00335K.

[11] M. Amde, Y. Yin, D. Zhang, J. Liu, Methods and recent advances in speciation analysis of mercury chemical species in environmental samples: a review, Chem. Speciat. Bioavailab. 28 (2016) 51–65. doi:10.1080/09542299.2016.1164019.

[12] V. Camel, Solid phase extraction of trace elements, Spectrochim. Acta Part B At. Spectrosc. 58 (2003) 1177–1233. doi:10.1016/s0584-8547(03)00072-7.

[13] G. Xin, Z. Chuguang, J. Zexiang, T. Zhiyong, Studies on the determination of mercury by on-line solvent extraction and non-aqueous media hydride generation non-dispersive atomic fluorescence spectrometry, Microchim. Acta. 148 (2004) 221–225. doi:10.1007/s00604-004-0264-9.

[14] N. Biçak, S. Sungur, M. Gazi, N. Tan, Selective liquid-liquid extraction of mercuric ions by octyl methane sulfonamide, Sep. Sci. Technol. 38 (2003) 201–217. doi:10.1081/SS-120016706.

[15] I. Karadjova, S. Arpadjan, J. Cvetković, T. Stafilov, Sensitive method for trace determination of mercury in wines using electrothermal atomic absorption spectrometry, Microchim. Acta. 147 (2004) 39–43. doi:10.1007/s00604-004-0216-4.

[16] D. Leyva, J. Estévez, A. Montero, I. Pupo, Sub-ppm determination of Hg and Cr in water: Cr speciation, X-Ray Spectrom. 36 (2007) 355–360. doi:10.1002/xrs.983.

[17] M. Vircavs, A. Peine, V. Rone, D. Vircava, Oxidation product of ammonium pyrrolidin-1-yldithioformate as a coprecipitator for the preconcentration of vanadium, cobalt, zinc, arsenic, iron, cadmium, selenium and mercury from aqueous solution, Analyst. 117 (1992) 1013–1017. doi:10.1039/an9921701013.

[18] A. Krata, K. Pyrzyńska, E. Bulska, Use of solid-phase extraction to eliminate interferences in the determination of mercury by flow-injection CV AAS, Anal. Bioanal. Chem. 377 (2003) 735–739. doi:10.1007/s00216-003-2148-y.

[19] J. Margetínová, P. Houserová-Pelcová, V. Kubáň, Speciation analysis of mercury in sediments, zoobenthos and river water samples by high-performance liquid chromatography hyphenated to atomic fluorescence spectrometry following preconcentration by solid phase extraction, Anal. Chim. Acta. 615 (2008) 115–123. doi:10.1016/j.aca.2008.03.061.

[20] Z. Fan, Hg(II)-imprinted thiol-functionalized mesoporous sorbent micro-column preconcentration of trace mercury and determination by inductively coupled plasma optical emission spectrometry, Talanta. 70 (2006) 1164–1169. doi:10.1016/j.talanta.2006.03.021.

[21] Y. Guo, B. Din, Y. Liu, X. Chang, S. Meng, M. Tian, Preconcentration of trace metals with 2-(methylthio)aniline-functionalized XAD-2 and their determination by flame atomic absorption spectrometry, Anal. Chim. Acta. 504 (2004) 319–324. doi:10.1016/j.aca.2003.10.059.

[22] M.A.H. Hafez, I.M.M. Kenawy, M.A. Akl, R.R. Lashein, Preconcentration and separation of total mercury in environmental samples using chemically modified chloromethylated polystyrene-PAN (ion-exchanger) and its determination by cold vapour atomic absorption spectrometry, Talanta. 53 (2001) 749–760. doi:10.1016/S0039-9140(00)00524-5.

[23] Karthika C, Sekar M, Removal of Hg (II) ions from aqueous solution by Acid Acrylic Resin A Study through Adsorption isotherms Analysis, I Res. J. Environ. Sci. 1 (2012) 34–41. doi:10.1086/507012.

[24] M. Daye, B. Ouddane, J. Halwani, M. Hamze, Preconcentration of Total Mercury from River Water by Anion Exchange Mechanism, Anal. Sci. 29 (2013) 955–961. doi:10.2116/analsci.29.955.

[25] A.H. El-Sheikh, Y.S. Al-Degs, R.M. Al-As'ad, J.A. Sweileh, Effect of oxidation and geometrical dimensions of carbon nanotubes on Hg(II) sorption and preconcentration from real waters, Desalination. 270 (2011) 214–220. doi:10.1016/j.desal.2010.11.048.

[26] Z. Es'haghi, G.R. Bardajee, S. Azimi, Magnetic dispersive micro solid-phase extraction for trace mercury pre-concentration and determination in water, hemodialysis solution and fish samples, Microchem. J. 127 (2016) 170–177. doi:10.1016/j.microc.2016.03.005.

[27] E.M. Soliman, M.B. Saleh, S.A. Ahmed, New solid phase extractors for selective separation and preconcentration of mercury (II) based on silica gel immobilized

aliphatic amines 2-thiophenecarboxaldehyde Schiff's bases, Anal. Chim. Acta. 523 (2004) 133–140. doi:10.1016/j.aca.2004.07.002.

[28] E.D.M. Massena Ferreira, R.J.A. L'Amour, J.M.N. Carmo, J.L. Mantovano, M.S. De Carvalho, Determination of Hg from Cu concentrates by X-ray fluorescence through preconcentration on polyurethane foam, Microchem. J. 78 (2004) 1–5. doi:10.1016/j.microc.2004.02.015.

[29] S. Arpadjan, L. Vuchkova, E. Kostadinova, Sorption of Arsenic, Bismuth, Mercury, Antimony, Selenium and Tin on Dithiocarbamate Loaded Polyurethane Foam as a Preconcentration Method for Their Determination in Water Samples by Simultaneous Inductively Coupled Plasma Atomic Emission Spectrometry and Electrothermal Atomic Absorption Spectrometry, Analyst. 122 (1997) 243–246. doi:10.1039/A606917G

[30] X. Zhou, C.J. Liu, Three-dimensional Printing for Catalytic Applications: Current Status and Perspectives, Adv. Funct. Mater. 27 (2017) 1701134. doi:10.1002/adfm.201701134.

[31] Z.X. Rao, B. Patel, A. Monaco, Z.J. Cao, M. Barniol-Xicota, E. Pichon, M. Ladlow, S.T. Hilton, 3D-Printed Polypropylene Continuous-Flow Column Reactors: Exploration of Reactor Utility in SNAr Reactions and the Synthesis of Bicyclic and Tetracyclic Heterocycles, European J. Org. Chem. 2017 (2017) 6499–6504. doi:10.1002/ejoc.201701111.

[32] A.S. Díaz-Marta, C.R. Tubío, C. Carbajales, C. Fernández, L. Escalante, E. Sotelo, F. Guitián, V.L. Barrio, A. Gil, A. Coelho, Three-Dimensional Printing in Catalysis: Combining 3D Heterogeneous Copper and Palladium Catalysts for Multicatalytic Multicomponent Reactions, ACS Catal. 8 (2018) 392–404.

doi:10.1021/acscatal.7b02592.

[33] P.J. Kitson, G. Marie, J.P. Francoia, S.S. Zalesskiy, R.C. Sigerson, J.S. Mathieson, L. Cronin, Digitization of multistep organic synthesis in reactionware for on-demand pharmaceuticals, Science. 359 (2018) 314–319. doi:10.1126/science.aao3466.

[34] M. Konarova, W. Aslam, L. Ge, Q. Ma, F. Tang, V. Rudolph, J.N. Beltramini, Enabling Process Intensification by 3 D Printing of Catalytic Structures, ChemCatChem. 9 (2017) 4132–4138. doi:10.1002/cctc.201700829.

[35] B.C. Gross, J.L. Erkal, S.Y. Lockwood, C. Chen, D.M. Spence, Evaluation of 3D printing and its potential impact on biotechnology and the chemical sciences, Anal. Chem. 86 (2014) 3240–3253. doi:10.1021/ac403397r.

[36] U. Kalsoom, P.N. Nesterenko, B. Paull, Current and future impact of 3D printing on the separation sciences, TrAC - Trends Anal. Chem. 105 (2018) 492–502. doi:10.1016/j.trac.2018.06.006.

[37] B. Gross, S.Y. Lockwood, D.M. Spence, Recent Advances in Analytical Chemistry by 3D Printing, Anal. Chem. 89 (2017) 57–70. doi:10.1021/acs.analchem.6b04344.

[38] S. Dupin, O. Lame, C. Barrès, J.Y. Charmeau, Microstructural origin of physical and mechanical properties of polyamide 12 processed by laser sintering, Eur. Polym. J. 48 (2012) 1611–1621. doi:10.1016/j.eurpolymj.2012.06.007.

[39] S.F.S. Shirazi, S. Gharehkhani, M. Mehrali, H. Yarmand, H.S.C. Metselaar, N. Adib Kadri, N.A.A. Osman, A review on powder-based additive manufacturing for tissue engineering: Selective laser sintering and inkjet 3D printing, Sci. Technol. Adv. Mater. 16 (2015) 33502. doi:10.1088/1468-6996/16/3/033502.

[40] M. Yan, X. Tian, G. Peng, Y. Cao, D. Li, Hierarchically porous materials prepared by

selective laser sintering, Mater. Des. 135 (2017) 62–68. doi:10.1016/j.matdes.2017.09.015.

[41] E. Lahtinen, L. Kivijärvi, R. Tatikonda, A. Väisänen, K. Rissanen, M. Haukka, Selective Recovery of Gold from Electronic Waste Using 3D-Printed Scavenger, ACS Omega. 2 (2017) 7299–7304. doi:10.1021/acsomega.7b01215.

[42] E. Lahtinen, M.M. Hänninen, K. Kinnunen, H.M. Tuononen, A. Väisänen, K. Rissanen, M. Haukka, Porous 3D Printed Scavenger Filters for Selective Recovery of Precious Metals from Electronic Waste, Adv. Sustain. Syst. 2 (2018) 1800048. doi:10.1002/adsu.201800048.

[43] E. Lahtinen, R. Precker, M. Lahtinen, E. Hey-Hawkins, M. Haukka, Selective Laser Sintering of Metal-Organic Frameworks: Production of Highly Porous Filters by 3D Printing onto a Polymeric Matrix, Chempluschem. (2019). doi:10.1002/cplu.201900081.

[44] M.R. Sohrabi, Preconcentration of mercury(II) using a thiol-functionalized metal-organic framework nanocomposite as a sorbent, Microchim. Acta. 181 (2014) 435–444. doi:10.1007/s00604-013-1133-1.

[45] U.S. Environmental Protection Agency, Definition and Procedure for the Determination of the Method Detection Limit—Revision 2, 2016.

[46] P. Diviš, M. Leermakers, H. Dočekalová, Y. Gao, Mercury depth profiles in river and marine sediments measured by the diffusive gradients in thin films technique with two different specific resins, Anal. Bioanal. Chem. 382 (2005) 1715–1719. doi:10.1007/s00216-005-3360-8.

[47] P. Pelcová, H. Dočekalová, A. Kleckerová, Development of the diffusive gradient in

thin films technique for the measurement of labile mercury species in waters, Anal. Chim. Acta. 819 (2014) 42–48. doi:10.1016/J.ACA.2014.02.013.

[48] M.S. Joens, C. Huynh, J.M. Kasuboski, D. Ferranti, Y.J. Sigal, F. Zeitvogel, M. Obst, C.J. Burkhardt, K.P. Curran, S.H. Chalasani, L.A. Stern, B. Goetze, J.A.J. Fitzpatrick, Helium Ion Microscopy (HIM) for the imaging of biological samples at sub-nanometer resolution, Sci. Rep. 3 (2013) 3514. doi:10.1038/srep03514.

[49] A. Fakhri, Investigation of mercury (II) adsorption from aqueous solution onto copper oxide nanoparticles: Optimization using response surface methodology, Process Saf. Environ. Prot. 93 (2015) 1–8. doi:10.1016/j.psep.2014.06.003.

[50] J. Ramkumar, T. Mukherjee, Selectivity Coefficient and Ion Exchange Isotherm in Inamuddin, M. Luqman, (Eds.), Ion Exchange Technology I: Theory and Materials, Springer Science & Business Media, 2012, pp. 44–48. http://link.springer.com/10.1007/978-94-007-4026-6

[51] T. Şahan, F. Erol, Ş. Yılmaz, Mercury(II) adsorption by a novel adsorbent mercapto-modified bentonite using ICP-OES and use of response surface methodology for optimization, Microchem. J. 138 (2018) 360–368. doi:10.1016/j.microc.2018.01.028.

[52] P. Cañada Rudner, J.M. Cano Pavón, F. Sánchez Rojas, A. Garcia De Torres, Use of flow injection cold vapour generation and preconcentration on silica functionalized with methylthiosalicylate for the determination of mercury in biological samples and sea-water by inductively coupled plasma atomic emission spectrometry, J. Anal. At. Spectrom. 13 (1998) 1167–1171. doi:10.1039/A803472I.

[53] R.M. Blanco, M.T. Villanueva, J.E.S. Uría, A. Sanz-Medel, J.E.S. Uría, A. Sanz-Medel, Field sampling, preconcentration and determination of mercury species in river waters, Anal. Chim. Acta. 419 (2000) 137–144. doi:10.1016/S0003-2670(00)01002-3.

[54] I. Dakova, I. Karadjova, V. Georgieva, G. Georgiev, Ion-imprinted polymethacrylic microbeads as new sorbent for preconcentration and speciation of mercury, Talanta. 78 (2009) 523–529. doi:10.1016/j.talanta.2008.12.005.

[55] R. Thomas, Practical Guide to ICP-MS : A Tutorial for Beginners, 3rd ed., CRC Press, Boca Raton, 2013.

Captions to figures

Fig. 1. SLS 3D printed 5 mm (diam. 16.5 mm) 3D-Thiol filter (left) and filter placed in a syringe (right).

Fig. 2. HIM image showing the attachment of the thiol-functionalized silica particle onto the 3D printed PA12 framework (left). HIM image of the overall macroporous structure of the 3D printed filter containing 10 wt% of functionalized silica on the PA12 framework. Thiol-functionalized silica particles are highlighted for clarity.

1 Fig. 1

2 

3

4 Fig. 2

5 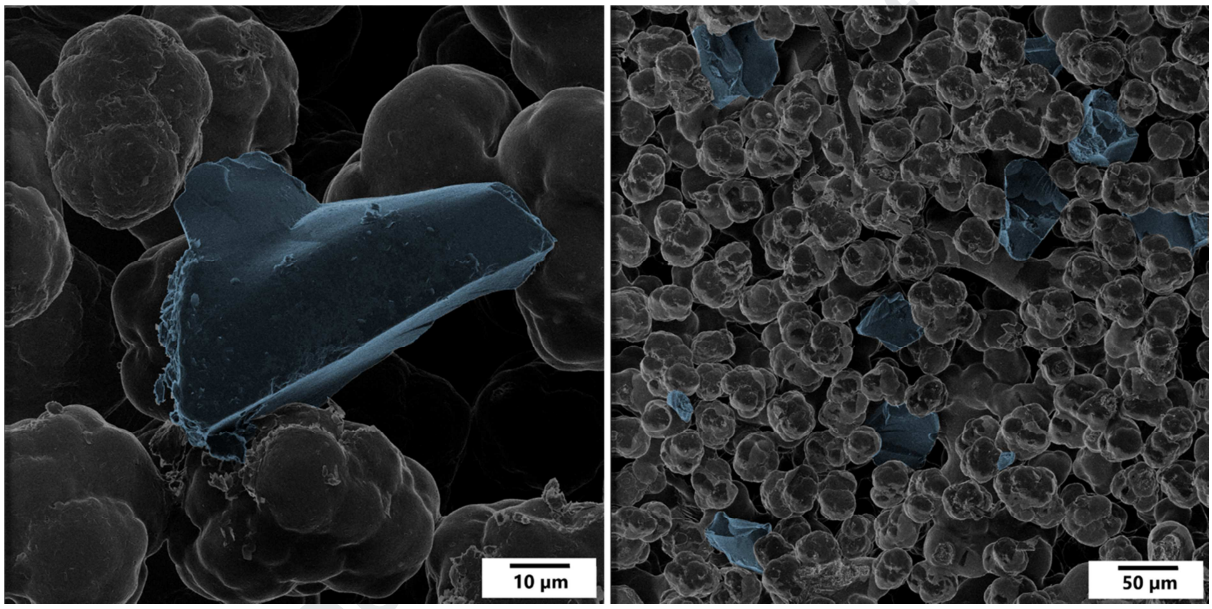

6

1 **Table 1.** ICP-MS instrumental operating parameters and conditions

System/ Operating parameter	Type/Value/Mode
Sample introduction	ESI prepFAST
Nebulizer	PFA-ST nebulizer for prepFAST
Spray chamber	Baffled cyclonic, glass, cooled to 2 °C
RF power	1600 W
Plasma gas flow rate	18 L min^{-1}
Auxiliary gas flow rate	1.2 L min^{-1}
Nebulizer gas flow rate	0.89–0.93 L min^{-1}
Isotope	The sum of ^{200}Hg, ^{201}Hg, and ^{202}Hg
Internal standard	^{193}Ir at 100 µg L^{-1} with 10 ms dwell time
Detector mode	Dual
Sweeps/reading	50
Replicates	5
Dwell time	100 ms
Scan mode	Peak hopping
Curve type	Linear through zero

2

3

Table 2. Constants of examined isotherms for Hg adsorption

Isotherm model	Constants	Value for 3D-Thiol (n=1)	The average value for Thiol (n=3)
Langmuir	q_{max} (mg g^{-1})	222.4	253.5
	K_L (L mg^{-1})	0.160	0.337
	R^2	0.975	0.940
Freundlich	K_F (L g^{-1})	23.5	54.2
	n	1.53	2.07
	R^2	0.982	0.980

Table 3. Recovery (%) ± std. deviation for Hg from 3D-Thiol using different eluent compositions

Eluent	Recovery (%)	Required dilution factor for analysis
0.3% thiourea in 8% HCl	90.1 ± 3.8	2.67
1% thiourea in 8% HCl	99.7 ± 4.9	5
2% thiourea in 10% HCl	98.8 ± 2.9	10
2% thiourea in 20% HCl	104.0 ± 3.7	13.33
0.3% thiourea in 40% HCl	105.1 ± 2.7	13.33
2% thiourea in 40% HCl	101.3 ± 4.2	13.33

Table 4. Average Hg concentration (ng L^{-1}) ± std. deviation for 20 ng L^{-1} spike to different matrices (n=3)

Sample	3D-Thiol method	Direct determination
Tap water[b]	23.27 ± 0.90	19.36 ± 0.45
Lake water 1[c]	20.75 ± 1.46	15.23 ± 0.40
Lake water 2	20.81 ± 1.88	13.08 ± 0.09
River water	21.24 ± 3.96	12.02 ± 1.01
Pond water 1[a,b]	18.96 ± 1.43	12.67 ± 0.44

[a]filtered with Whatman No. 41, [b]two 3D-Thiol filters, [c]n=2

Table 5. Average Hg concentration (ng L^{-1}) ± std. deviation for different water samples with the 3D-Thiol method and direct determination (n=3)

Sample	3D-Thiol method	Direct determination
Tap water	0.61 ± 0.06	<MDL
Groundwater	0.34 ± 0.02	<MDL
Lake water 1	0.94 ± 0.09	<MDL
Lake water 2	1.79 ± 0.13	<MDL
River water[a,b]	1.39 ± 0.08	<MDL
Pond water 1[a]	0.61 ± 0.12	<MDL
Pond water 1[a,b]	0.65 ± 0.04	<MDL
Pond water 2	2.94 ± 0.12	4.44 ± 0.12

[a]filtered with Whatman No. 41, [b]two 3D-Thiol filters

Table 1. ICP-MS instrumental operating parameters and conditions

System/ Operating parameter	Type/Value/Mode
Sample introduction	ESI prepFAST
Nebulizer	PFA-ST nebulizer for prepFAST
Spray chamber	Baffled cyclonic, glass, cooled to 2 °C
RF power	1600 W
Plasma gas flow rate	18 L min^{-1}
Auxiliary gas flow rate	1.2 L min^{-1}
Nebulizer gas flow rate	0.89–0.93 L min^{-1}
Isotope	The sum of ^{200}Hg, ^{201}Hg, and ^{202}Hg
Internal standard	^{193}Ir at 100 µg L^{-1} with 10 ms dwell time
Detector mode	Dual
Sweeps/reading	50
Replicates	5
Dwell time	100 ms
Scan mode	Peak hopping
Curve type	Linear through zero

Table 2. Constants of examined isotherms for Hg adsorption

Isotherm model	Constants	Value for 3D-Thiol (n=1)	The average value for Thiol (n=3)
Langmuir	q_{max} (mg g^{-1})	222.4	253.5
	K_L (L mg^{-1})	0.160	0.337
	R^2	0.975	0.940
Freundlich	K_F (L g^{-1})	23.5	54.2
	n	1.53	2.07
	R^2	0.982	0.980

Table 3. Recovery (%) ± std. deviation for Hg from 3D-Thiol using different eluent compositions

Eluent	Recovery (%)	Required dilution factor for analysis
0.3% thiourea in 8% HCl	90.1 ± 3.8	2.67
1% thiourea in 8% HCl	99.7 ± 4.9	5
2% thiourea in 10% HCl	98.8 ± 2.9	10
2% thiourea in 20% HCl	104.0 ± 3.7	13.33
0.3% thiourea in 40% HCl	105.1 ± 2.7	13.33
2% thiourea in 40% HCl	101.3 ± 4.2	13.33

Table 4. Average Hg concentration (ng L^{-1}) ± std. deviation for 20 ng L^{-1} spike to different matrices (n=3)

Sample	3D-Thiol method	Direct determination
Tap water[b]	23.27 ± 0.90	19.36 ± 0.45
Lake water 1[c]	20.75 ± 1.46	15.23 ± 0.40
Lake water 2	20.81 ± 1.88	13.08 ± 0.09
River water	21.24 ± 3.96	12.02 ± 1.01
Pond water 1[a,b]	18.96 ± 1.43	12.67 ± 0.44

[a]filtered with Whatman No. 41, [b]two 3D-Thiol filters, [c]n=2

Table 5. Average Hg concentration (ng L^{-1}) ± std. deviation for different water samples with the 3D-Thiol method and direct determination (n=3)

Sample	3D-Thiol method	Direct determination
Tap water	0.61 ± 0.06	<MDL
Groundwater	0.34 ± 0.02	<MDL
Lake water 1	0.94 ± 0.09	<MDL
Lake water 2	1.79 ± 0.13	<MDL
River water[a,b]	1.39 ± 0.08	<MDL
Pond water 1[a]	0.61 ± 0.12	<MDL
Pond water 1[a,b]	0.65 ± 0.04	<MDL
Pond water 2	2.94 ± 0.12	4.44 ± 0.12

[a]filtered with Whatman No. 41, [b]two 3D-Thiol filters

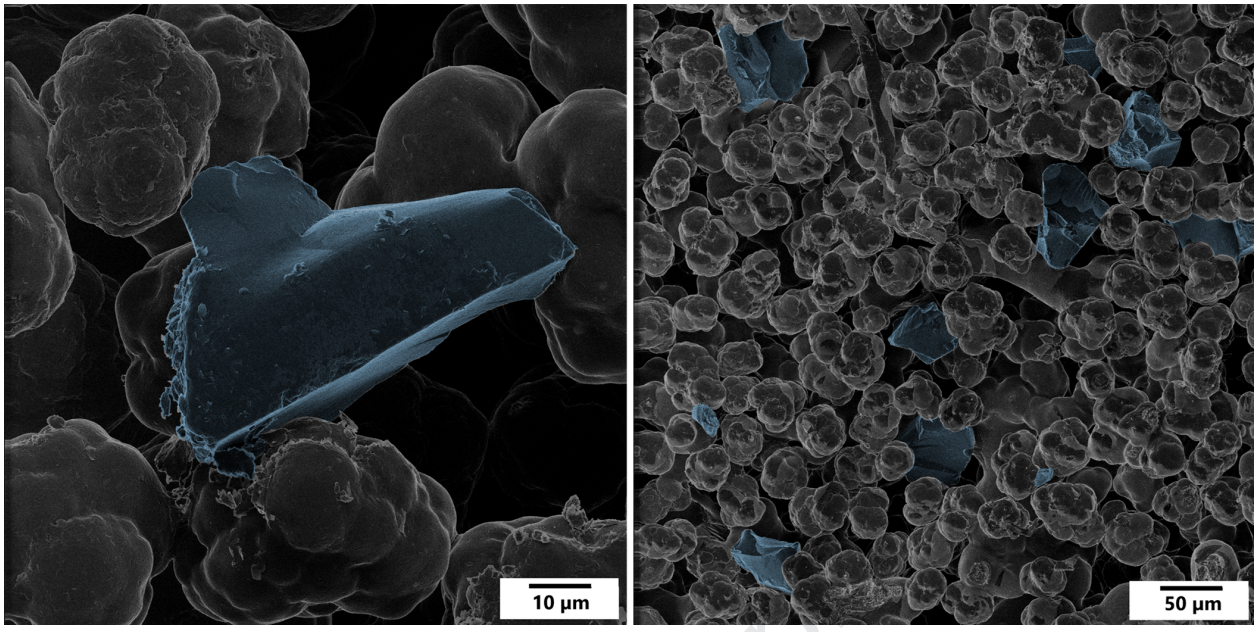

Highlights

- Highly selective and accurate preconcentration method for Hg
- Hg adsorption onto 3D printed metal scavenger and elution with acidic thiourea solution
- Accurate Hg determination at picogram level in natural waters with a preconcentration factor of 92.8
- Determination of background concentrations in natural water with ICP-MS

Declaration of interests

☒ The authors declare that they have no known competing financial interests or personal relationships that could have appeared to influence the work reported in this paper.

☐The authors declare the following financial interests/personal relationships which may be considered as potential competing interests: